Ecological Indicators 54 (2015) 116–123

Contents lists available at ScienceDirect

Ecological Indicators

journal homepage: www.elsevier.com/locate/ecolind

Developing and applying novel spectral feature parameters for classifying soil salt types in arid land

Pingbin Jin [a], Pingheng Li [b], Quan Wang [c,*], Zhi Pu [b]

[a] Department of Geosciences, Zhejiang University, Hangzhou 310027, China
[b] Xinjiang Institute of Ecology and Geography, CAS, Urumqi 830011, China
[c] Graduate School of Agriculture, Shizuoka University, Shizuoka 422-8529, Japan

ARTICLE INFO

Article history:
Received 27 June 2014
Received in revised form 6 January 2015
Accepted 17 February 2015

Keywords:
Arid land
Soil salinity
Salt type
Hyperspectral
Feature parameter
Classification algorithm

ABSTRACT

Soil salinization is a major desertification process that threatens especially the stability of arid ecosystems. There is an urgent need for intensive monitoring and quick assessment of salinization through remote sensing as a tool for combating desertification in such ecosystems. Recent researches have revealed that in order to retrieve soil salt contents accurately from hyperspectral reflectance, a pre-knowledge of salt types is required, which greatly outlines the spectral features of saline soil reflectance. In this study, a set of feature parameters have been developed after a thorough investigation of spectral responses to different soil salt types and salt contents for quick and accurate classification of soil salt types. The application has been validated using three independent datasets composed from: laboratory experiments (dataset I), *in-situ* field measurements (dataset II), and satellite-borne Hyperion image (dataset III). For comparison, four other common classification algorithms have been validated using the same datasets. The results showed that the new approach proposed in this study performed well with not only single-type but also multiple-type salts for which the four common algorithms performed rather fairly. Furthermore, validating using datasets II and III showed that the newly proposed approach had a stable performance while the other four failed, indicating the advantage of the new approach. The feature parameters developed in this study hence provide a novel and efficient approach for salt type classification from reflectance spectra, and we foresee its potential applications on large-scale soil salt type mapping towards better understanding soil salinity characterization from remote sensing data.

1. Introduction

Soil salinization is one of the most common land degradation processes in arid and semi-arid regions (Richards, 1954; FAO, 1988), where accumulated soluble salts in the soil, influences soil properties and the environment, and hence affecting soil productivity (Mahmoud et al., 2009). Typically, saline soils are highly erosive and have poor structure, low fertility, low microbial activity, and other attributes not conducive for plant growth (Masoud et al., 2006). To enhance sustainable agricultural management in arid and semi-arid environments, timely and proper decisions on combating soil salinization must be achieved through early identification and monitoring of salt-affected areas.

Remote sensing offers a quick and efficient tool for soil salinization identification and monitoring (Wang et al., 2012a). Compared with expensive, time-consuming and intensive sampling requirements of traditional techniques for identifying and monitoring soil salinization, high revisiting frequency and large spatial coverage of remote sensing data offers incomparable advantages on understanding spatiotemporal variations of soil salinity. In the past decade, remote sensing has been used widely to investigate soil salinity (Ben-Dor et al., 2002; Dehaan and Taylor, 2002, 2003; Metternicht and Zinck, 2003; Farifteh et al., 2006, 2008; Mahmoud et al., 2009; Wang et al., 2012a). These ranged from simple visual interpretation of hardcopy satellite images to sophisticated spectral unmixing and multivariate linear and non-linear techniques (Dehaan and Taylor, 2002, 2003; Farifteh et al., 2007).

Despite the existence of numerous studies, application of remote sensing data in salinity studies remains a mounting challenge. In nature, saline soils commonly contain different salt types which greatly affects soil reflectance and may therefore cause

* Corresponding author. Tel.: +81 54 2383683.
E-mail address: aqwang@ipc.shizuoka.ac.jp (Q. Wang).

http://dx.doi.org/10.1016/j.ecolind.2015.02.028
1470-160X/

significant errors during soil salt content estimation (Wang et al., 2012b). Several earlier studies have tried to deal with this dilemma. For instance, based on laboratory control experiments with different salt types and content levels, Howari et al. (2002) reported that different salt types exhibit completely different spectrum curves. Our previous study had shown that the soil spectra of different salt types are very different and even greater than the differences caused by different salt content levels of a single salt type, indicating that accurate retrieval of soil salt content requires prior identifying the salt types (Wang et al., 2012b). However, whether the recent efforts in modeling and classification techniques are able to overcome this limitation and provide a relatively accurate method in salinity studies remains a challenge. Farifteh et al. (2008) tried to identify different soil salt types using two spectral identification algorithms (PIMA and TSG), based on statistical methods identifying an unknown mineral from a reference library, but obtained low accuracy. Although there are a number of algorithms available for classification, they usually require complex statistical processes and very few studies have ever reported success for soil salt type classification.

Parameters of spectral features may offer another approach for soil salt type classification. Feature parameters generally can represent the main feature characteristics of the entire wavelength domain but with high-adaptability to spectral resolution and with high-sensitivity to a given specific property (Kokaly and Clark, 1999). Therefore, use of spectral feature parameters may provide a simple and faster alternative for property-understanding including classification. There are many studies that have used varied spectral feature parameters (in some studies called shape parameters or feature characteristics) in retrieving vegetation and soil properties such as chlorophyll (Baranoski and Rokne, 2005; le Maire et al., 2004), vegetation water content (Curran et al., 2001; Mutanga et al., 2005), environmental stress (Clevers et al., 2004; Kooistra et al., 2004) and so. For soil properties, several attempts have been achieved by use of varied spectral feature parameters (such as the position, depth, width, area). These included soil composition (Van der Meer, 2004; Xu et al., 2008), soil grain size (Ghrefat et al., 2007), soil rubification (Ben-Dor et al., 2006), soil moisture (Demattê et al., 2006; Lobell and Asner, 2002), and soil salinity (Taylor, 2004; Farifteh et al., 2008), but few on soil salt types. Since feature parameters have several advantages on applications, such as their simple forms, their ability to represent the main feature characteristics of entire wavelengths, their high-adaptability to spectral resolution, and their high-sensitivity to specific parameter (Kokaly and Clark, 1999), it is foreseen that they may offer a quick and easy way also on soil salt type classification.

This paper aimed at developing novel spectral feature parameters that are specifically oriented to providing simple and quick classification of soil salt types based on hyperspectral reflected information. Such feature parameters are identified and generalized *via* thorough investigations on reflected spectra collected from soils treated with different salt types and concentrations in laboratory. They are further validated using *in situ* field-measured data (dataset II) and hyperspectral image data obtained by the satellite-borne Hyperion sensor (dataset III). In addition, for comparison, the current commonly applied classification techniques in remote sensing studies, *e.g.* mostly maximum likelihood (Jia and Richards, 1994; Gopinath, 1998), *k*-nearest neighbor (Denœux, 2008; Franco-Lopez et al., 2001), support vector machine (Cortes and Vapnik, 1995; Vapnik, 1998) and artificial neural network (Hammerstrom, 1993; Nurnberger et al., 2002), are applied for classifying soil salt types. All the four techniques have been widely applied in many studies, such as land cover, crops, natural vegetation, soil characteristics (Mucherino et al., 2009) with remote sensing imagery, or hyperspectral measurements etc., but with few studies on soil salt types.

2. Materials and methods

2.1. Laboratory experiment, field sampling, and different datasets

2.1.1. Controlled laboratory experiment (Dataset I)

Spectral data of artificial soils with different soil salt types and salinity were measured in laboratory. Typical non-saline surface soil (soil salt content of ca. 0.154% as determined in laboratory later) from Sanggong River watershed (43°09′45°29″N, 87°47′88°17″E) in Xinjiang, China, was collected and moved to laboratory (see Fig. 1 for the watershed location and sampling strategy). The watershed covers a drainage area of 1670 km^2 and experiences a continental type of climate with an average annual rainfall of 220 mm and an average annual temperature of 6.9 °C (Luo et al., 2003). The alluvial plain in our sampling site has a fine-textured soil (sandy loam with sand of 44.37%, silt of 42.68%, and clay of 12.95%) (Wang et al., 2012a). The soil samples were air-dried, crushed, and passed through a 2-mm sieve to form the base soil for further experiments. Thereafter, the samples were treated with different salts and corresponding spectral data were taken in the laboratory.

The salt minerals mainly responsible for salinity of soil are found within three chemical groups, *i.e.*, carbonates, halides, and sulphates. Therefore, pure NaCl, Na_2CO_3 and Na_2SO_4 in solutions were used to produce three single-type and three salt mixtures ($NaCl + Na_2CO_3$, $NaCl + Na_2SO_4$, and $Na_2CO_3 + Na_2SO_4$) at various salinities. For three single-type salt groups, 7 different levels of salt concentration by weight of dry soil was assigned for each saline soil treatment, which has been replicated three times. While for the three salt mixtures, different proportions of the given two salts were set ranging at 1:9, 3:7, 5:5, 7:3, and 9:1. For each proportion, 5 different levels of soil salt content from 7 g/kg to 200 g/kg were examined with three replicates, resulted in a total of 75 measurements for three composite groups. Reflected spectra were taken using an ASD spectroradiometer covering wavelengths from 350 to 2500 nm (ASD FR, ASD, USA). Detail description of experiments can be found in Wang et al. (2012a).

2.1.2. Field in situ measurements (Dataset II)

The Dataset II composed different salt types, salinity, and other soil properties as well as reflected spectra taken using ASD spectroradiometer *in situ* in field. In total 31 sampled sites were collected in May 2009 inside the watershed across the alluvial plain (oasis) in the low reaches where soil salinization frequently occurs (see Fig. 1 for locations). Each composite sampled site consisted of five subsamples collected within a 90×90 m grid, and the position was determined with a GPS unit. After soil reflected spectra were measured *in situ* in the field, the composite topsoil samples were collected and taken to laboratory for analysis of soil chemical and physical properties (including soil moisture, electrical conductivity, pH, concentrations of eight soluble salt ions, and total soluble salt content). Detail description of spectra measurements and soil sampling can also be found in Pu (2010) and Wang et al. (2012a).

2.1.3. Satellite-born data (Dataset III)

An additional dataset retrieved from a Hyperion image dated on May 12, 2009 covering the sampling area as well as within the period of field measurements was compiled for further analysis. Hyperion image was processed through various procedures as detailed in Pu (2010) before being used to retrieve satellite-borne hyperspectral reflectance for each sampled sites. Procedures included destriping, smile effect correction, atmospheric correction, as well as geometrical correction (Goodenough et al., 2003; Kruse et al., 2003). Atmospheric correction was based on the FLAASH module inside ENVI software. Geometrical correction has been based on a geo-referenced TM scene using 16 ground control points (GCPs) and obtained an RMSE of 0.44 m. Satellite-borne

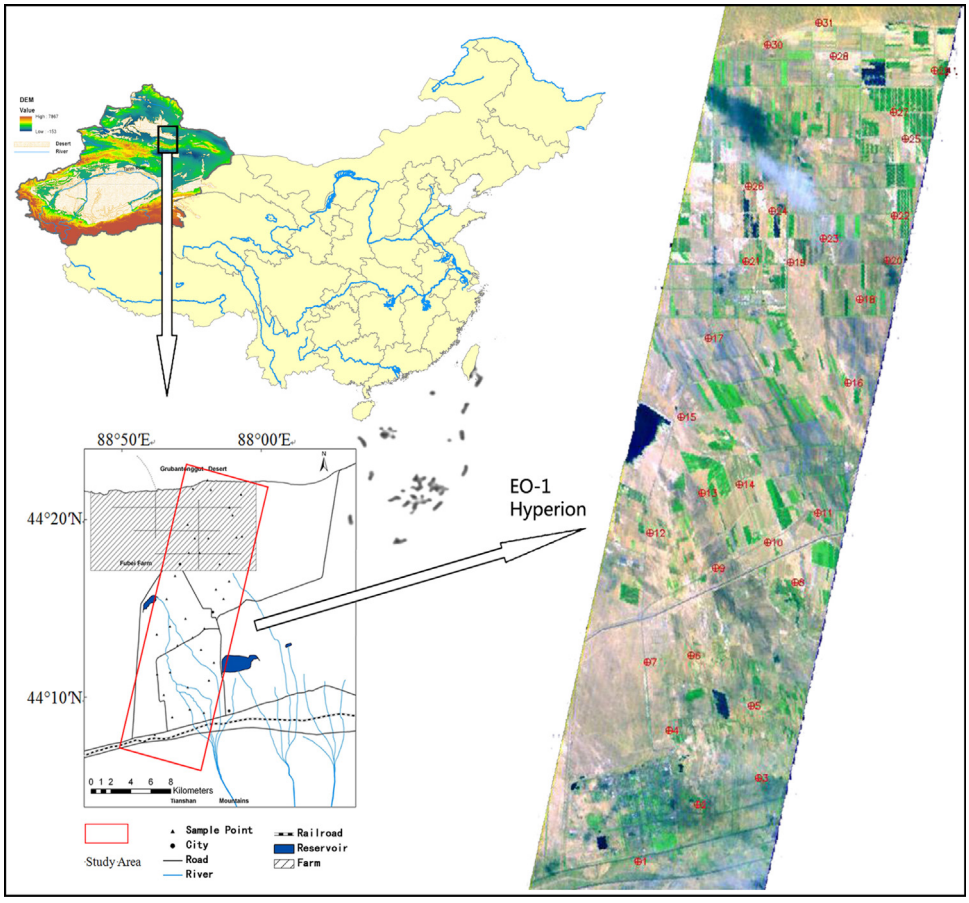

Fig. 1. Study location and sampling strategy. In total 31 sampled sites were selected inside Sanggong watershed across the alluvial plain (oasis) in the low reaches. Each composite sampled site consisted of five subsamples collected within a 90 × 90 m grid. The background image was from the Hyperion data acquired on May 12, 2009 when field measurements were taken.

reflectance spectra were then extracted from all available 176 (8–57, 79–120, 128–166, 179–223) bands after having removed noisy bands and two overlapped bands (VNIR 56–57 and SWIR 77–78) from the original 242 spectral bands of Hyperion at the 31 sampling sites based on their GPS locations (Pu, 2010).

2.2. Spectral feature parameters for soil salt type classification

Spectral feature parameters are generally designed from the band position, depth, width, or area that specifically responds to a given property under examination. They are widely applied in remote sensing studies for their simple and quick identification of a given property, *e.g.* the red edge inflection point (REIP) (Dawson and Curran, 1998). However, to the best of our knowledge, there is no report of such feature parameters for rapid soil salt type classification. Consequently, we have generalized a new set of feature parameters, namely, α and R_{mean}, for achieving this task, following the work by Wang et al. (2013). The pattern parameter α (identical to α_1 in Wang et al., 2013) is defined as the angle of line 1 (reflectance at 350 nm to the peak reflectance within the domain of 750 to 850 nm) with line 2 (the peak reflectance of 750–850 nm to the peak reflectance from 1800 to 2200 nm). The other parameter R_{mean} refers to the mean reflectance value of the entire wavelength domain from 350 nm to 2500 nm (see Fig. 2 for definitions). This two parameters are simple, easy to calculate but with high sensitivity to different salt types and can adapt to different spectral resolutions.

The pattern parameter α was found to be mainly determined by salt types ($P = 0 < 0.001$). As reported by Wang et al. (2013), α was confined to a specific range of [107.7°, 129.6°], [129.6°, 134.7°], and [134.7°, 169.0°], corresponding to spectra of Na_2CO_3, Na_2SO_4, and NaCl type of saline soils, respectively, with only very few overlapped cases under high salt contents (Fig. 3a and b). Statistical test revealed that salt content did not significantly affect this pattern parameter ($P > 0.5$), since varying the salt contents only led the changes in the confined range that corresponded to salt types (Wang et al., 2013).

The parameter R_{mean} was also found to be sensitive to salt types ($P < 0.001$). As revealed in Fig. 3a, R_{mean} decreased with increased

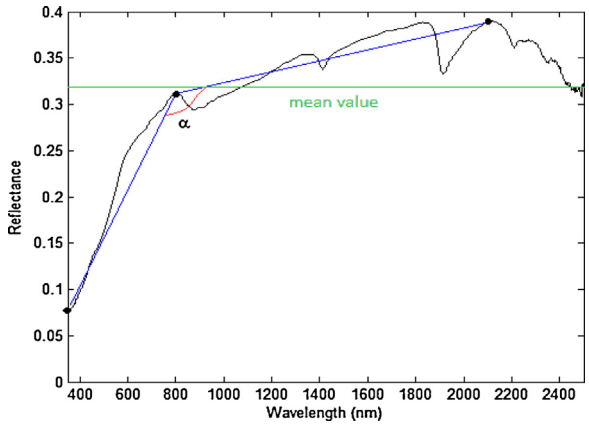

Fig. 2. Definitions of two spectral feature parameters (α and R_{mean}). α is identical to α_1 in Wang et al. (2013).

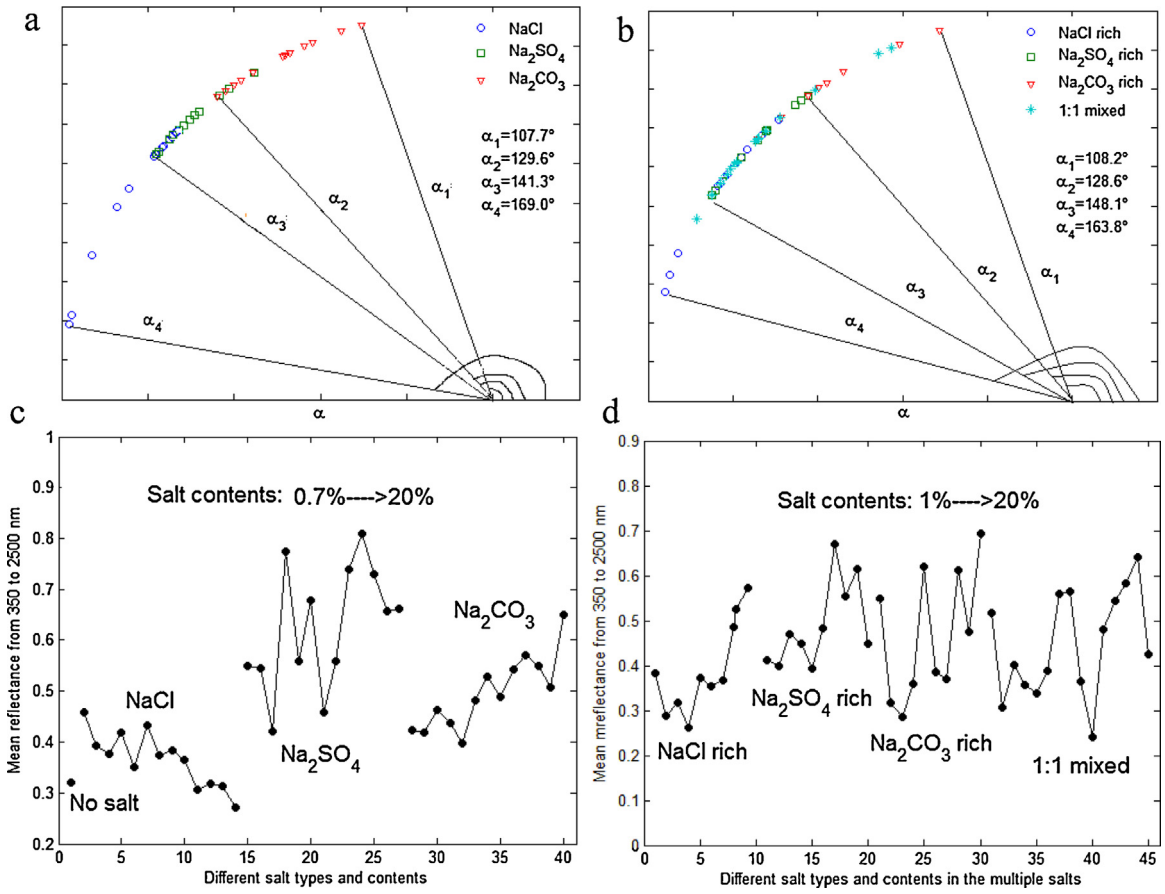

Fig. 3. Confines and variations of the two spectral feature parameters with different salt types and contents.

concentration levels of NaCl type of saline soils while an inverse trend was identified for Na_2CO_3 type of saline soils. However, such pattern did not hold for Na_2SO_4 type of saline soils. Similarly, no clear trend of R_{mean} with concentration levels can be distinguished with composite salts (Fig. 3d). Even so, the values of R_{mean} in the boundary of two salt types separated by parameter α had a large difference, where one side was larger than 0.5 while the other side was lower than 0.5 (Fig. 3c and d). Therefore, the parameter R_{mean} can be added to compliment classification judgment of the parameter α, to reduce the probability of false classification of salt types.

2.3. Soil salt type classification

Since both parameters α and R_{mean} are sensitive to different salt types, we designed a new approach to classify salt types using the soil reflectance data based on the set of parameters, as shown in Fig. 4: when $\alpha > 142$, or $136 < \alpha < 142$ and $R_{mean} < 0.5$, the sample was classified as NaCl type; when $136 < \alpha < 142$ and $R_{mean} > 0.5$, or $130 < \alpha < 136$, or $125 < \alpha < 130$ and $R_{mean} > 0.5$, the sample was classified as Na_2SO_4 type; when $125 < \alpha < 130$ and $R_{mean} < 0.5$, or $\alpha < 125$, the sample was classified as NaCl type. R_{mean} values of field ground-based measured spectra and satellite-borne spectra are commonly lower than that in the laboratory measured spectra, thus we applied 0.4 for dataset II and 0.3 for dataset III in this study.

For comparison, four typical classification algorithms that have been widely validated and applied, namely, Maximum likelihood (Richards, 1993), *k*-nearest neighbor (Denœux, 2008; Franco-Lopez, 2001), Support vector machine (Vapnik, 1998), and artificial Neural network (Wilkes and Wade, 1997), were also examined in this study for salt type classification. For each algorithm, twenty percent of the distinctive dataset I were used for training, while the other eighty percent for validation.

Performance evaluation of different classification algorithms was based on the confusion matrix, from which a series of descriptive and analytical statistics been derived (Foody, 2002). In this study, three typical parameters (Accuracy, Reliability, and Kappa Coefficient) that widely been applied in classification assessment were used (Congalton, 1991). They were calculated from the error matrix of each classification accordingly (Congalton, 1991).

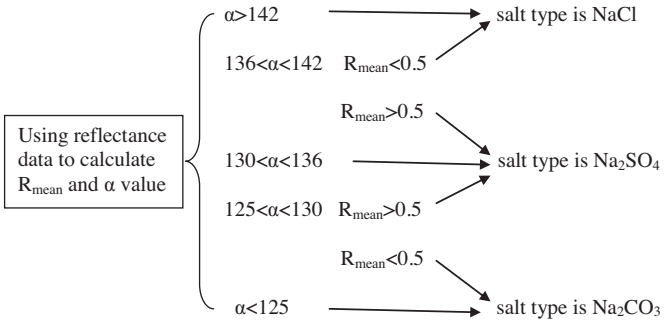

Fig. 4. Classification algorithms for soil saline types based on spectral pattern parameters.

3. Results

3.1. Classification results using dataset I (controlled laboratory experiment)

3.1.1. Single-type salts

For all five classification algorithms (maximum likelihood, *k*-nearest neighbor, support vector machine, neural network, and the spectral feature parameters), Table 1 has summarized their classification accuracies and reliabilities for the three single-type salts that formed dataset I. Perfect performance with an accuracy of 100% for classifying NaCl was obtained from all the commonly applied algorithms except the spectral feature parameters proposed in this study, which obtained reliable (84.6% accuracy) but inferior to the other four counterparts. Again, the poorest performance of the proposed method on classifying Na_2SO_4 was noted compared with the best performance of support vector machine at 84.6%. However, the best performance for classifying Na_2CO_3 was obtained for the spectral feature method which had an accuracy of 85.7%. On reliability basis, *k*-nearest neighbor was found to be most reliable for NaCl classification (92.3% accuracy), while the neural network method was best for Na_2SO_4 (100%) and the newly proposed spectral feature parameters for Na_2CO_3 in the meantime. Considering salt types, the NaCl type had the largest classification accuracy, but was relatively inferior in accuracy for the other two salt types (ranging from 61.5% to 92.3%). The reliabilities of all five methods on three single salt types were similar (80% on average). Overall, the results indicated that all the five methods had similar high classification accuracy and reliability judging only from Kappa coefficients (k, all >0.68).

3.1.2. Composite salt mixtures

Low performances were observed for all the commonly applied classification algorithms except the newly proposed approach in case of salt mixtures, as indicated in Table 2. All four commonly applied classification algorithms obtained 65% to 75% of classification accuracies for NaCl rich salts, compared with their 100% accuracies for the single type of NaCl salt. Much larger drop of classification accuracy was found for Na_2SO_4 rich type of soils, where the accuracies varied from 25.0% to 45.0% for the four commonly applied classification algorithms. Furthermore, they generally had classification accuracies below 25.0% for Na_2CO_3 rich soils type. The level of reliability also dropped to 40s% (from 41.9% of support vector machine to 46.4% of maximum likelihood) for NaCl-rich soil, while 25.0% to 45.0% for Na_2SO_4 rich type of soils, and 28.6% to 62.5% for the Na_2CO_3 rich type. The Kappa coefficients were decreased from >0.7 to be less than 0.20 for all the four commonly applied algorithms.

On the other hand, for all soils with salt mixtures, the new approach produced the best performance among all algorithms examined. For NaCl-rich type of soils, the classification based on feature parameters reached an accuracy of 80.0%. Similar accuracy (75.0%) was obtained for Na_2SO_4-rich type of soils. Even if the accuracy was found to decrease to 60.0% for Na_2CO_3-rich type of soils, it remained the best for all algorithms and nearly 3 times better than that of *k*-nearest neighbor method. Its reliability was 64.0%, 68.2%, 92.3%, for NaCl, Na_2SO_4 and Na_2CO_3-rich type of soils, respectively. The Kappa coefficient of the newly proposed method remained high (k = 0.58) for different types of salt soils.

When soils with multiple-type composite salts are considered, the NaCl-rich type soils can be well classified (85% by the new method, and 65.0–75.0% by the other four commonly applied methods), while for the other two composite multiple-salt types had less accurate classifications except when the newly proposed method was used (60.0–75.0% by the new method, 20.0–45.0% by the other four typical methods). Similar low reliability of the three mixed salts was obtained when the four typical methods were used (40% on average), while that of the newly proposed method was much higher (64.0%, 68.2%, 92.3% for NaCl-rich, Na_2SO_4-rich and Na_2SO_4-rich salt types, respectively).

3.2. Classifications using datasets II and III (with field in situ measured spectra and extracted from Hyperion images)

Both datasets (II and III) had same soil salt types and other soil properties, but reflected spectra were different. The spectra contained in dataset II were taken *in situ* in the field, while those in dataset III were retrieved from simultaneous Hyperion image covering the sampling region. Laboratory analysis revealed that the dominant negative ion of the collected 31 soil samples was SO_4^{2-} (87.85% of total negative ions, see Table 3 for the results of concentrations of eight soluble salt ions of all samples) followed by Cl^- (9.13%) while the dominant cation was Na^+ (81.47% of total positive ions, see Table 3) followed by Ca^{2+} (10.87%). Hence, the soil types contained in both datasets were dominated by Na_2SO_4 and most of them should be classified as Na_2SO_4—rich multiple salts.

Table 4 summarized the classification results of all five classification methods using datasets II and III. The results showed that all the four commonly applied classification methods failed to predict the salt type, such that most of the samples were misclassified to NaCl-type, leading to very low classification accuracies (all less than 20%). While the newly proposed approach, on the other hand, consistently gave good classification results for both datasets (with an accuracy of 61.3% for dataset II and 45.2% for dataset III), indicating its wide application for field soil salt classification.

4. Discussion

Salt minerals within three chemical groups, namely carbonates, halides, and sulphates, are mainly responsible for salinity of soils (Richards, 1954). Salt minerals in nature are rarely pure, since trace elements are often trapped in crystal lattices during crystallization and thus affect the spectral properties of saline soils (Hunt and Salisbury, 1970). Howari et al. (2002) and Farifteh et al. (2008) revealed that different salt types have very different spectrum curves based on laboratory control experiments with different salt types and several salt content levels. Using similar laboratorial approach, Wang et al. (2012b) confirmed that soil spectra of different salt types were very different and revealed that the difference due to different salt types even greater than the differences caused by different salt content levels. They also argued that for accurate retrieval of soil salt content from reflected spectra, it is paramount to classify the salt types (Wang et al., 2013).

As a common approach, soil salt types and salinity are determined through laboratory analysis of soil samples collected in the field on the eight soluble salt ions concentrations, which is costly, time consuming and only with point information. Therefore new approaches such as optical remote sensing are necessary for detecting salt types more efficiently. Although remote sensing has been widely used for collecting information on soil salinity in the past decades (Ben-Dor et al., 2002; Metternicht and Zinck, 2003; Taylor et al., 1994, 2001), few studies attempted to highlight salt types' effects on soil spectra or classify different salt types from remotely sensed data. Farifteh et al. (2008) had attempted to identify the different salt types using two spectral identification algorithm (PIMA and TSG) but with poor accuracy. Hence, remote sensing technique remains a major challenge for quickly detection of soil salt types despite its importance in monitoring soil salinization.

Various spectral feature parameters (such as the absorption position, depth, width, area) derived from spectra have been widely applied in remote sensing studies to retrieval many subjects,

Table 1
Summarized results of the salt type classify of the three single salt types using 5 different classification methods.

Method	Accuracy			Reliability			Kappa Coefficient
	NaCl (%)	Na_2SO_4 (%)	Na_2CO_3 (%)	NaCl (%)	Na_2SO_4 (%)	Na_2CO_3 (%)	
I	100	76.9	81.8	69.2	81.2	83.3	0.73
II	100	69.2	71.4	76.9	92.9	81.8	0.73
III	100	84.6	81.8	69.2%	86.7	84.6	0.77
IV	100	76.9	84.6	84.6	81.3	100	0.81
V	84.6	61.5	85.7	92.3	78.6	72.7	0.69

Method I: maximum likelihood; II: *k*-nearest neighbor; III: support vector machine; IV: neural network; V: the reflectance shape parameters method.

Table 2
Summarized results of the salt type classify of the three multiple salts types.

Method	Accuracy			Reliability			Kappa Coefficient
	NaCl rich (%)	Na_2SO_4 rich (%)	Na_2CO_3 rich (%)	NaCl rich (%)	Na_2SO_4 rich (%)	Na_2CO_3 rich (%)	
I	65.0	45.0	25.0	46.4	50.0	35.7	0.18
II	70.0	25.0	20.0	43.8	35.7	28.6	0.08
III	65.0	35.0	25.0	41.9	43.8	38.5	0.13
IV	75.0	40.0	25.0	45.5	42.1	62.5	0.20
V	80.0	75.0	60.0	64.0	68.2	92.3	0.58

Method I: maximum likelihood; II: *k*-nearest neighbor; III: support vector machine; IV: neural network; V: the reflectance shape parameters method.

Table 3
Summary of salt types and salt content of the 31 *in situ* field soil samples.

Ion content (g/kg)	Negative ion				Positive ion				EC 1:5 (ms/cm)	SSC (g/kg)
	CO_3^{2-}	HCO_3^-	Cl^-	SO_4^{2-}	Ca^{2+}	Mg^{2+}	K^+	Na^+		
Proportion%	0.25	2.77	9.13	87.85	10.87	2.56	5.10	81.47	–	–
Mean	0.02	0.21	0.68	6.51	0.39	0.09	0.18	2.92	2.63	1.12
Max.	0.15	0.36	2.79	30.43	1.13	0.47	0.4	13.68	9.97	4.69
Min.	0.00	0.08	0.02	0.25	0.00	0.01	0.04	0.14	1.90	1.03
SD	0.03	0.06	0.79	7.17	0.36	0.11	0.09	3.29	2.44	1.13

ranging from vegetation parameters (Baranoski and Rokne, 2005; Clevers et al., 2004; Curran et al., 2001; Kooistra et al., 2004; le Maire et al., 2004; Mutanga et al., 2005) to soil properties (Ben-Dor et al., 2006; Demattê et al., 2006; Farifteh et al., 2008; Ghrefat et al., 2007; Lobell and Asner, 2002; Taylor, 2004; Van der Meer, 2004; Xu et al., 2008). For soil salinity, Taylor (2004) described how the shape of the hydroxyl absorption feature at 2200 nm (depth and width) changes with increased salinity (hydroxyl depth versus width). Apart from usually focused absorption position, depth, width and area types of feature parameters, Hill and Schuett (2000) proposed to parameterize the shape of the reflectance continuum in the range of 0.35 to 1.4 μm to estimate soil organic matter concentration. This was based on the fact that the specific influence of organic matter on spectral reflectance is not expressed in narrow absorption bands but determined by the overall shape of the reflectance in that domain. Since different salts with similar absorption bands exhibits very different overall shapes, the approach by Hill and Schuett (2000) was followed to classify soil salt types where feature parameters are used to describe the overall spectral shape rather than specific absorption feature (*e.g.* position, depth, width, area).

Statistical analysis revealed that the feature parameter α was mainly determined by salt types ($P = 0 < 0.001$). As shown in Fig. 3a and b, the α values of single salt types or multiple-type composite salt types generally produced different ranges with marginal overlaps among different salt types resulted from varied salt contents, which may produce some misclassifications between the boundaries of salt types. To compliment for it, another parameter R_{mean} was proposed based on the fact that soils with overlaps of α often exhibit large different values of R_{mean}. Combination of both α and R_{mean} can therefore reduce the probability of miss-classification. In addition, R_{mean} may also be helpful for bridging the gaps between laboratory analysis and field application, as R_{mean} values in field or satellite-borne are generally lower compared in laboratory controlled environments for being affected by soil moisture or other factors. By properly reducing the R_{mean} threshold can improve classification accuracy and practical application of this method in field.

Table 4
Summarized results of the salt type classify of dataset II and III.

Method	Dataset II				Dataset III			
	NaCl	Na_2SO_4	Na_2CO_3	Accuracy (%)	NaCl	Na_2SO_4	Na_2CO_3	Accuracy (%)
I	25	4	2	12.90	27	2	2	6.45
II	22	3	6	9.68	28	1	2	3.23
III	23	2	6	6.45	29	1	1	3.23
IV	21	6	4	19.35	25	5	1	16.13
V	10	19	2	61.3	16	14	1	45.2

Method I: maximum likelihood; II: *k*-nearest neighbor; III: support vector machine; IV: neural network; V: the reflectance shape parameters method.

Apparently, commonly applied classification algorithms performed well with single type salt soils, especially for NaCl and Na_2SO_4 types because distinctive spectra are generally associating with soils with a specific type of salt. However, this is not the case for soils with multiple types of salts. All commonly applied algorithms failed to work with soils containing multiple types of salts if judged from Kappa coefficients, especially when containing NaCl. We note that even with a small proportion of NaCl, commonly applied algorithms generally classified them as NaCl type saline soils, regardless of the proportions of being occupied either by Na_2CO_3 or Na_2SO_4 in these soils. This therefore caused a large number of Na_2SO_4 rich and Na_2CO_3 rich soils to be incorrectly assigned as NaCl rich type. On the other hand, the new approach is not only applicable to single salt types but also to the mixed salts, as proven from the high classification accuracy (reached 80.0%, 75.0%, and 60.0% for NaCl-rich, Na_2SO_4-rich and Na_2CO_3-rich soils, respectively) and a fairly good overall Kappa coefficient ($k = 0.6$).

Furthermore, the newly proposed approach is the only method that can be easily applied under field conditions as indicated from the validation results from datasets II and III. For field collected spectra and soil samples, the newly proposed approach obtained an accuracy of >60% (dataset II). Decreased accuracy was found when satellite-borne parameters were used primarily due to the atmospheric correction errors, even though it is the only method that had an accuracy of 45%. It is conceivable that the accuracy could be improved on satellite-borne remote sensing data with better atmospheric corrections and hence paving way for rapid retrieval of saline type information for large spatial area. However, we realized that validations solely based on datasets II and III were not enough since the soil samples collected from field were only dominated by one type of salt (Na_2SO_4). Extensive validations with other dominant types of saline soils are required in the future studies.

In this approach, it is also noteworthy that NaCl type saline soils are generally classified better than other soils, since soils with other saline types are mistakenly classified as NaCl type but seldom with NaCl type saline soils. The reason may be due to the similarity of spectra of NaCl saline and salt-free base soils. This leads to incorrect identification of Na_2CO_3 and Na_2SO_4 types saline soils as NaCl type. Similar trend was found for multiple-type saline soils with gradual reduction in classification accuracies from NaCl rich to Na_2SO_4 and Na_2CO_3—rich types of saline soils. This may probably due to the stronger effects of NaCl on spectra than the other types of salts and hence leading to incorrect classifications even with Na_2SO_4 rich and Na_2CO_3 rich saline soils. Since the spectra of saline soils with small amount of Cl^- ion tend to be identical to NaCl-rich, common classification methods may fail to distinguish them. On the contrary, the new approach developed in this study is based on spectral features that are highly sensitive to salt types and thus have high potential for application in saline soil classification. This novel approach should be helpful for improving soil salinity retrieval as well for its ability in providing saline type information.

5. Conclusions

Remote sensing offers a rapid and inexpensive approach to monitor and assess soil salinization in arid land. Although soil salinity has been retrieved directly from hyperspectral reflectance, recent studies have revealed that a pre-knowledge of salt types plays an important role on retrieval accuracy of soil salinity since soil saline types greatly shapes spectral features of saline soil reflectance. However, commonly applied classification algorithms such as neuron network, support vector machine among others have all failed to provide saline type information directly from hyperspectral reflectance and hence a challenge still exists for remote sensing applications on soil salinization. The novel spectral feature parameters method developed in this study is specifically oriented to solve this dilemma. Generalized from laboratory experiments, the set of parameters were validated using field collected samples and proved their sensitivities to saline types. Further extension of using satellite-borne feature parameters has also been validated using field data. As a fair performance was obtained even with satellite-borne data, the newly proposed method may therefore pave a way for rapid retrieval of saline type information from satellite recorded reflectance, and the accuracy is foreseen to improve with better atmospheric corrections. However, extensive validation of the new method especially with various saline type soils is still required to enhance its wide application.

Acknowledgements

This study was supported by the “973” Program (2012CB956204), the CAS project (grant no. 1074041001), and the NSFC project (No. 41371364).

References

Baranoski, G.V.G., Rokne, J.G., 2005. A practical approach for estimating the red edge position of plant leaf reflectance. Int. J. Remote Sens. 26, 503–521.
Ben-Dor, E., Patkin, K., Banin, A., Karnieli, A., 2002. Mapping of several soil properties using DAIS-7915 hyperspectral scanner data. A case study over soils in Israel. Int. J. Remote Sens. 23, 1043–1062.
Ben-Dor, E., Levin, N., Singer, A., Karnieli, A., Braun, O., Kidron, G.J., 2006. Quantitative mapping of the soil rubification process on sand dunes using an airborne hyperspectral sensor. Geoderma 131, 1–21.
Clevers, J.G.P.W., Kooistra, L., Salas, E.A.L., 2004. Study of heavy metal contamination in river floodplains using the red-edge position in spectroscopic data. Int. J. Remote Sens. 25, 3883–3895.
Congalton, R.G., 1991. A review of assessing the accuracy of classifications of remotely sensed data. Remote Sens. Environ. 37, 35–46.
Cortes, C., Vapnik, V., 1995. Support-vector networks. Mach. Learn. 20, 273–297.
Curran, P.J., Dungan, J.L., Peterson, D.L., 2001. Estimating the foliar biochemical concentration of leaves with reflectance spectrometry testing the Kokaly and Clark methodologies. Remote Sens. Environ. 76, 349–359.
Dawson, T.P., Curran, P.J., 1998. A new technique for interpolating the reflectance red edge position. Int. J. Remote Sens. 19, 2133–2139.
Dehaan, R.L., Taylor, G.R., 2002. Field-derived spectra of salinized soils and vegetation as indicators of irrigation-induced soil salinization. Remote Sens. Environ. 80, 406–417.
Dehaan, R., Taylor, G.R., 2003. Image-derived spectral end members as indicators of salinisation. Int. J. Remote Sens. 24, 1043–1062.
Demattê, J.A.M., Sousa, A.A., Alves, M.C., Nanni, M.R., Fiorio, P.R., Campos, R.C., 2006. Determining soil water status and other soil characteristics by spectral proximal sensing. Geoderma 135, 179–195.
Denœux, T., 2008. A k-nearest neighbor classification rule based on Dempster–Shafer theory. Studies in Fuzziness and Soft Computing. Classic Works of the Dempster–Shafer Theory of Belief Functions, vol. 219. Springer, pp. 737–760.
FAO, 1988. Salt-affected soils and their management. In: FAO, Soils Bulletin, 39. Food and Agriculture Organization of the United Nations, Rome.
Farifteh, J., Farshad, A., George, R.J., 2006. Assessing salt-affected soils using remote sensing, solute modelling, and geophysics. Geoderma 130, 191–206.
Farifteh, J., Van der Meer, F., Atzberger, C., Carranza, E.J.M., 2007. Quantitative analysis of salt-affected soil reflectance spectra: a comparison of two adaptive methods (PLSR and ANN). Remote Sens. Environ. 110, 59–78.
Farifteh, J., van der Meer, F., van der Meijde, M., Atzberger, C., 2008. Spectral characteristics of salt-affected soils: a laboratory experiment. Geoderma 145, 196–206.
Foody, G.M., 2002. Status of land cover classification accuracy assessment. Remote Sens. Environ. 80, 185–201.
Franco-Lopez, H., Ek, A.R., Bauer, M.E., 2001. Estimation and mapping of forest stand density, volume, and cover type using the k-nearest neighbors method. Remote Sens. Environ. 77, 251–274.
Ghrefat, H.A., Goodell, P.C., Hubbard, B.E., Langford, R.P., Aldouri, R.E., 2007. Modeling grain size variations of aeolian gypsum deposits at White Sands New Mexico, using AVIRIS imagery. Geomophology 88, 57–68.
Goodenough, D.G., Dyk, A., Niemann, K.O., Pearlman, J.S., Chen, H., Han, T., Murdoch, M., West, C., 2003. Processing Hyperion and ALI for forest classification. IEEE Trans. Geosci. Remote Sens. 6, 1321–1331.
Gopinath, R.A., 1998. Maximum likelihood modeling with Gaussian distributions for classification. Acoustics, Speech and Signal Processing, Proceedings of the 1998 IEEE International Conference vol. 2, 661–664.
Hammerstrom, D., 1993. Working with neural networks. IEEE Spectr. 307, 46–53.
Hill, J., Schuett, B., 2000. Mapping complex patterns of erosion and stability in dry Mediterranean ecosystems. Remote Sens. Environ. 74, 557–569.
Howari, F.M., Goodell, P.C., Miyamoto, S., 2002. Spectral properties of salt crusts formed on saline soils. J. Environ. Qual. 31, 1453–1461.

Hunt, G.R., Salisbury, J.W., 1970. Visible and near-infrared spectra of minerals and rocks. I. Silicate minerals. Modern Geol. 1, 283–300.
Jia, X., Richards, J.A., 1994. Efficient maximum likelihood classification for imaging spectrometer data sets. IEEE Trans. Geosci. Remote Sens. 32, 274–281.
Kokaly, R.F., Clark, R.N., 1999. Spectroscopic determination of leaf biochemistry using band-depth analysis of absorption features and stepwise multiple linear regression. Remote Sens. Environ. 67, 267–287.
Kooistra, L., Salas, E.A.L., Clevers, J.G.P.W., Wehrens, R., Leuven, R.S.E.W., Nienhuis, P.H., Buydens, M.C., 2004. Exploring field vegetation reflectance as an indicator of soil contamination in river floodplains. Environ. Pollut. 127, 281–290.
Kruse, F.A., Boardman, J.W., Huntington, J.F., 2003. Comparision of airborne hyperspectral data and EO-1 Hyperion for mineral mapping. IEEE Trans. Geosci. Remote Sens. 6, 1388–1400.
le Maire, G., François, C., Dufrêne, E., 2004. Towards universal deciduous broad leaf chlorophyll indices using PROSPECT simulated database and hyperspectral reflectance measurements. Remote Sens. Environ. 89, 1–28.
Lobell, D.B., Asner, G.P., 2002. Moisture effects on soil reflectance. Soil Sci. Soc. Am. J. 66, 722–727.
Luo, G., Chen, X., Zhou, K., Ye, M., 2003. Temporal and spatial variation and stability of the oasis in the Sangong River Watershed, Xinjiang. China. Sci. China (Ser D) 46, 62–73.
Mahmoud, A.A., Shabbir, A.S., Yasser, R.O., 2009. Soil salinity mapping model developed using RS and GIS—a case study from Abu Dhabi, United Arab Emirates. Eur. J. Sci. Res. 26, 342–351.
Masoud, M., Patwardhan, A.M., Gore, S.D., 2006. A new methodology for producing of risk maps of soil salinity, Case study: Payab Basin, Iran. J Appl. Sci. Environ. Manage. 10, 9–13.
Metternicht, G.I., Zinck, J.A., 2003. Remote sensing of soil salinity: potentials and constraints. Remote Sens. Environ. 85, 1–20.
Mucherino, A., Petraq Pajorgi, Pardalos, P.M., 2009. A survey of data mining techniques applied to agriculture. Oper. Res. Int. J. 92, 121–140.
Mutanga, O., Skidmore, A.K., Kumar, L., Ferwerda, J., 2005. Estimating tropical pasture quality at canopy level using band depth analysis with continuum removal in the visible domain. Int. J. Remote Sens. 26, 1093–1108.
Nurnberger, A., Pedrycz, W., Kruse, R., 2002. Neural network approaches. In: Klosgen, W., Zytkow, J.M. (Eds.), Handbook of Data Mining and Knowledge Discovery. Oxford University Press, New York, NY, pp. 304–317.
Pu, Z., 2010. Quantitative Retrieval of Saline Soil Salt Content in Arid Region Using Hyperspectral Data—Take the Sangong River Watershed as a Case. Xinjiang Institute of Ecology and Geography, Chinese Academy of Sciences, Urumqi, pp. 113 (PhD dissertation).
Richards, J.A., 1993. Remote Sensing Digital Image Analysis: An Introduction, second ed. Springer, ISBN 0-387-5480-8.
Richards, L.A., 1954. Diagnosis and Improvement of Saline and Saline and Alkali Soils (Agricultural Handbook No. 60). US Department of Agricultural, US Government Printing Office, Washington, DC.
Taylor, G.R., Bennett, B.A., Mah, A.H., Hewson, R.D., 1994. Spectral properties of salinised land and implications for interpretation of 24 channel imaging spectrometry. Proceedings of First International Remote Sensing Conference and Exhibition, Strasbourg, France, 504–513.
Taylor, G.R., Hemphill, P., Currie, D., Broadfoot, T., Dehaan, R.I., 2001. Mapping dryland salinity with hyperspectral imagery. Proc. IEEE Int. Geosci. Remote Sens. Symp., IGARSS 1, 302–304, http://dx.doi.org/10.1109/IGARSS.2001.976138.
Taylor, G.R., 2004. Field and image spectrometry for soil mapping. In: Proceedings 12th Australian Remote Sensing Conference, Fremantle, WA, Australia.
Van der Meer, F., 2004. Analysis of spectral absorption features in hyperspectral imagery. Int. J. Appl. Earth Obs. Geoinf. 5, 55–68.
Vapnik, V., 1998. Statistical Learning Theory. Wiley, New York, NY.
Wang, Q., Li, P., Chen, X., 2012a. Modeling salinity effects on soil reflectance under various moisture conditions and its inversion application: a laboratory experiment. Geoderma 170, 103–111.
Wang, Q., Li, P., Chen, X., 2012b. Retrieval of soil salt content from an integrated approach of combining inversed reflectance model and regressions: an experimental study. IEEE Trans. Geosci. Remote Sens. 50, 3950–3957.
Wang, Q., Li, P., Maina, J.N., Chen, X., 2013. A study on the effects of how salt types greatly shaped soil reflectance spectra versus salt concentration. Commun. Soil Sci. Plant Anal. 44, 1503–1510.
Wilkes, A.L., Wade, N.J., 1997. Bain on neural networks. Brain Cognit. 33, 295–305.
Xu, D.Q., Ni, G.Q., Jiang, L.L., Shen, Y.T., Li, T., Ge, S.L., Shu, X.B., 2008. Exploring for natural gas using reflectance spectra of surface soils. Adv. Space Res. 41, 1800–1817.